Thermodynamics of Peptide−RNA Recognition: The Binding of a Tat Peptide to TAR RNA

Hemant Suryawanshi, Harshana Sabharwal, and Souvik Maiti*

Proteomics and Structural Biology Unit, Institute of Genomics and Integrative Biology, CSIR, Mall Road, Delhi 110 007, India

Received: January 4, 2010; Revised Manuscript Received: July 15, 2010

RNA−peptide interactions have been intensively studied at the structural level; however, in the absence of thermodynamic studies, the molecular forces that dictate the binding specificities and affinities remain elusive. Here we evaluate the thermodynamics (ΔG, ΔH, ΔS) of HIV-1 TAR RNA hairpin and Tat peptide interaction as well as the hydration changes that accompany these interactions, through a series of calorimetric, spectroscopic, and osmotic stress studies. Tat peptide binding enhances the thermal stability of the TAR RNA hairpin; however, the thermal enhancement decreases with increasing Na^+ concentration. The equilibrium association constant (K_a) is determined by fluorescence titrations and examined as a function of Na^+ concentration and temperature. The binding constant (K_a) decreases with increasing Na^+ concentration. The binding free energy (ΔG) is found to have a large nonpolyelectrolyte component with release of a single counterion upon binding. The ITC profiles showed two independent sites binding, indicating specific as well as nonspecific interactions. The enthalpy changes associated with both the binding sites are found to be more negative for the binding process at lower salt concentration of 20 mM Na^+. Our binding studies under osmotic stress conditions show that there is a release of 28 (±4) and 21 (±3) water molecules upon complex formation at 20 and 80 mM Na^+ concentration supporting the observed positive entropy contributions and accounting for discrepancies between ΔH_{cal} and ΔH_{vH}. In aggregate, our results suggest that the hydrogen bonding of arginine to TAR RNA dictates the binding interaction.

Introduction

Central to the functioning of the cell, RNA−protein interactions play a major role in numerous biological phenomena. To investigate the principles underlying RNA recognition, studies have been focused on models that employ RNA and peptide derived from their cognate proteins.[1–5] Understanding the RNA binding of peptides is imperative for elucidating their mode of binding and development of new and improved derivatives with better selectivity. On a fundamental level, RNA−peptide interaction offers a simple and well-defined system to understand principles that determine RNA recognition. Most studies involving peptide−RNA complexes are focused on arginine-rich peptide segments derived from phage and lentiviral regulatory systems.[1] Arginine-rich peptides appear to play a dominant role in RNA recognition due to their unique electrostatic and hydrogen bonding potential.[2–5] These model studies facilitate understanding of more complex peptide/protein−RNA interactions.

Over the past years, several efforts have provided structural data indicating adaptive binding of arginine-rich peptide motifs of bacteriophage antiterminator proteins, viral regulatory proteins, viral coat proteins, and ribosomal proteins and their cognate RNA.[6–19] Among these, HIV-1 TAR RNA and Tat-derived peptides represent a well-known and simple paradigm to study such interactions. HIV-1 TAR RNA exists as a hairpin and is located at the 5′ end of the viral mRNA transcript. Its secondary structure consists of two helical stem regions separated by a three-nucleotide bulge and a six-nucleotide apical loop capping the terminal stems.[20] Binding of the viral transcription factor Tat, which belongs to the arginine-rich family of RNA binding proteins, increases the lentiviral replication manifold by increasing the processivity of RNA polymerase II.[21] NMR studies have shown that TAR contains specific arginine binding sites in its major groove at base G26 and phosphates in the RNA backbone. Tat binding induces an arginine-binding pocket in RNA by extrusion of the three nucleotide bulges and coaxial stacking of the two stem helices. These conformational changes create potential for the formation of a U23-A-27:U38 base triplex.[6–8] The HIV-1 Tat peptide−TAR complex, formed by very few amino acid contacts of largely unstructured peptide which can also be viewed as a simple ligand, presents a highly attractive model for the study.

At present, there exists a large collection of high-resolution structural data involving a variety of RNA−peptide complexes. These structural studies are valuable for determining the mode and position of binding besides establishing three-dimensional shape of the complex. However, these studies alone are limiting as they do not provide information on the nature of molecular forces that drive complex formation and the relative contributions of the different molecular interactions. Therefore, to have a comprehensive view of these interactions, it is essential to complement these structural studies with detailed thermodynamic studies. Taking the minimum first steps in this direction, we for the first time present a detailed thermodynamic characterization of HIV-1 TAR RNA and Tat-derived arginine-rich peptide interaction using a combination of spectroscopic and calorimetric techniques.

Materials and Methods

The 15 mer Tat peptide (SYGRKKRRQRRRPPQ) was obtained from Hysel India Pvt. Ltd. and was used without any further purification. The 27 base fragment of the TAR RNA

* To whom correspondence should be addressed. E-mail: souvik@igib.res.in. Phone: +91-11-2766-6156. Fax: +91-11-2766-7471.

10.1021/jp1000545
Published on Web 08/05/2010

(CCAGAUCUGAGCCUGGGAGCUCUCUGG) was obtained from Sigma-Aldrich, Singapore. Concentration of RNA was determined optically at 260 nm at 25 °C using the molar extinction coefficient of 251.8×10^3 M^{-1} cm^{-1}. These values were calculated by extrapolation of the tabulated values of the dimer and monomer nucleotides at 25 °C to high temperatures using protocols reported previously.[22] Fluorescence-labeled RNA containing 2-aminopurine (2-AP) between two bulge bases (C and U) was purchased from Sigma-Aldrich. Mili-Q water was used in all the experiments. The other reagents were commercially available analytical grade and were used without further purification. All measurements were performed in 10 mM sodium cacodylate buffer containing 10 mM NaCl and 0.1 mM EDTA, pH 7.5.

CD Spectroscopy. CD spectra were recorded in a Jasco spectropolarimeter (model 715, Japan) equipped with a thermoelectrically controlled cell holder and a cuvette with a path length of 1 cm. CD spectra were recorded between 200 and 325 nm at 25 °C in 10 mM sodium cacodylate buffer, containing 10 mM NaCl and 0.1 mM EDTA at pH 7.5. Typically, in the titration experiments the RNA concentration was fixed at 5 μM, and the concentration of peptide ranged from 0 to 15 μM. The titration was finished when a significant decrease in the CD signal was not observed upon further addition of peptide.

Temperature-Dependent UV Spectroscopy (UV Melting). Thermal denaturation scans were obtained using a Cary 400 (Varian) spectrophotometer equipped with a thermoelectrically controlled cell holder. A quartz cell with 1 cm path length was used for all the absorbance studies. Absorbance versus temperature profiles were measured at 260 nm. The temperature ranged from 15 to 100 °C with a heating rate of 0.5 °C/min. In these thermal denaturation studies, the TAR RNA hairpin duplex concentration was kept at 1 μM, and peptide concentrations varied from 0 to 3 μM. The experiments were performed in 10 mM sodium cacodylate, 10 mM NaCl (pH 7.5), and 0.1 mM EDTA. For each optically detected transition, the melting temperature (T_m) was determined using previously described methods.[23]

Fluorescence Spectroscopy. Fluorescence spectra of the 2-aminopurine (2-AP) fluorescence labeled RNA were measured in a Fluoromax 4 (Spex) spectrofluorophotometer equipped with a thermoelectrically temperature-controlled cell holder (quartz cuvette, 1 cm × 1 cm). The excitation wavelength was set at 320 nm, and the emission spectra were recorded from 340 to 500 nm. The experiments were performed in 10 mM sodium cacodylate buffer (pH 7.5) containing varying amounts of NaCl concentration ranging from 10, 20, 30, 50, to 150 mM and 0.1 mM EDTA at 25 °C. Temperature-dependent titrations were also carried out at 10, 15, 20, and 25 °C at 10 and 70 mM NaCl (pH 7.5) to calculate the van't Hoff enthalpy change. Typically, in the titration experiments the RNA concentration was fixed at 100 nM, and the concentration of peptide varied from 0 to 400 nM. The changes in fluorescence intensity at 377 nm (maximum wavelength) were monitored as a function of peptide concentration. For data analysis, the observed fluorescence intensity was considered as the sum of the weighted contributions from a bound peptide and an unbound RNA form.

$$F = (1 - \alpha)F_0 + \alpha F_b \quad (1)$$

where F is the observed fluorescence intensity at each titrant concentration; F_0 and F_b are the respective fluorescence intensities of initial and final states of titration; and α is the mole fraction of RNA in bound form. Assuming 1:1 stoichiometry for the interaction, it can be shown that

$$\alpha^2[R]_0 - \alpha([R]_0 + [L]_t + 1/K_a) + [L]_t = 0 \quad (2)$$

where K_a is the association constant; $[R]_0$ is the total RNA concentration; and $[L]_t$ is the added peptide concentration. From eqs 1 and 2, it can be shown that

$$\Delta F = (\Delta F_{max}/2R_0) \times \{(R_0 + L_t + 1/K_a) \pm \sqrt{(R_0 + L_t + 1/K_a)^2 + 4R_0L_t}\} \quad (3)$$

where $\Delta F = F - F_0$ and $\Delta F_{max} = F_{max} - F_0$.

The free energy of binding was calculated from the standard relation $\Delta G = -RT \ln K_a$ where R is the universal gas constant and T is the absolute temperature in kelvin. The enthalpy changes ΔH were determined from the temperature dependence of equilibrium association constant where ΔH is the slope of the $\ln(K_a)$ vs $1/T$ plot according to the equation $\ln(K_a) = -(\Delta H/RT) + \Delta S/R$, where ΔS is the entropy change.

Salt Dependence of the Binding Constant. The effect of different NaCl concentrations on the 1:1 binding constants was examined at 25 °C and pH 7.5, by fluorescence titration experiments, as described above, and analyzed according to the polyelectrolyte theory by Record et al.[24] The observed salt dependence of the binding constants is explained by the following relationship

$$\delta \log K_a/\delta \log[Na^+] = -Z\psi = SK \quad (4)$$

where Z is the apparent charge on the ligand and Ψ is the proportion of counterions associated with each nucleic acid phosphate group. The slope (SK) of the plot, which is equivalent to the number of counterions released from RNA upon peptide binding, was obtained from lines of best linear least-squares fit and was used to evaluate the polyelectrolyte contribution (ΔG_{pe}) to the observed binding free energy (ΔG_{obs}) using the relationship

$$(\Delta G_{pe}) = (-SK)RT \ln[Na^+] \quad (5)$$

The nonpolyelectrolyte contribution was then given by the following equation[25]

$$(\Delta G_{obs}) = (\Delta G_{pe}) + (\Delta G_t) \quad (6)$$

Isothermal Titration Calorimetry (ITC). Isothermal calorimetric measurements were performed at 25 °C on a MicroCal VP-ITC (MicroCal, Inc.; Northampton MA) in 10 mM sodium cacodylate containing 10 mM NaCl and 0.1 mM EDTA at pH 7.5. In a typical experiment, 4 μL aliquots of 350 μM peptide were injected from a 250 μL rotating syringe (350 rpm) into an isothermal sample chamber containing 1.5 mL of a RNA solution that was 10 μM in strand. Each experiment of this type was accompanied by the corresponding control experiment in which 350 μM peptides were injected into a solution of buffer alone. The duration of each injection was 8.0 s, and the delay between injections was 300 s. The initial delay prior to the first injection was 200 s. Each injection generated a heat burst curve (microcalories per second vs seconds). The area under each

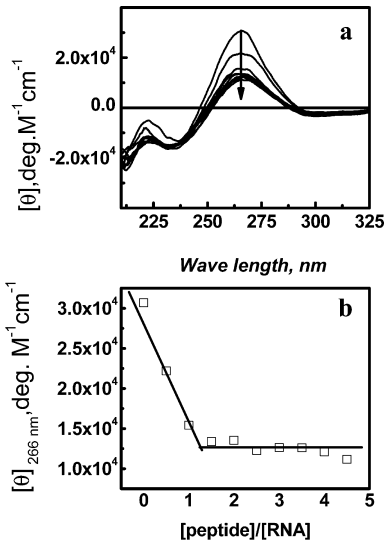

Figure 1. (a) Circular dichroism spectra (CD) of the Tat peptide−TAR RNA complexes. (b) CD titration curves detected at 265 nm for several [peptide]/[RNA] ratios in buffer consisting of 10 mM sodium cacodylate, 10 mM NaCl, and 0.1 Mm NaEDTA, at pH 7.5 and 25 °C. Molar ellipticities, $[\theta]$, are in units of deg M^{-1} cm^{-1}, where M refers to moles of RNA strand per liter. [RNA] = 5 μM.

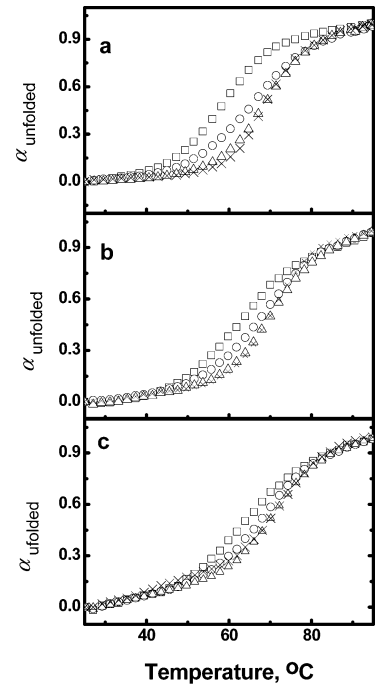

Figure 2. UV melting profiles at 260 nm for Tat peptide−TAR RNA complexes at the ratios of [peptide]/[RNA] of 0 (□), 1 (○), 2 (Δ), and 3 (×) under the solution conditions of 10 mM sodium cacodylate (pH 7.5) buffer consisting of (a) 20, (b), 40 and (c) 80 mM Na^+ concentration. [RNA] = 1 μM.

curve was determined by integration [using the Origin version 7.0 software (MicroCal, Inc.; Northampton, MA)] to obtain a measure of the heat associated with that injection. The net enthalpy change for the TAR RNA hairpin duplex and Tat peptide interaction was determined by subtraction of the heats of dilution.

Results and Discussion

Thermodynamic analysis of peptide binding to RNA offers valuable insight into the molecular forces involved in complex formation that cannot be obtained by structural studies alone. Understanding the contribution of different thermodynamic parameters is also essential in rational designing and development of peptides as future drugs. We have employed HIV-1 TAR RNA and Tat-derived peptide as a model system to investigate the principles critical to the binding event. A combination of spectroscopic and calorimetric techniques is used to generate a thermodynamic profile (ΔG, ΔH, ΔS) of the TAR RNA hairpin duplex−Tat peptide interaction.

Circular Dichroism Spectroscopy Studies. CD spectropolarimetry is a useful tool for detecting and characterizing the nucleic acid−ligand interactions. CD spectra allow detection of even slight conformational changes in the nucleic acid structures due to possible binding reactions. Figure 1a represents the CD spectra of 5 μM TAR RNA in the presence of varying amounts of peptide ranging from 0 to 15 μM in 10 mM sodium cacodylate buffer, pH 7.5. As depicted in Figure 1a, the spectrum of TAR RNA showed a strong positive peak at 265 nm, a strong negative peak at 210 nm, and a weak negative peak at 240 nm, thus reflecting the presence of the A-form of RNA. However, upon addition of the peptide to a solution of TAR RNA hairpin, substantial CD signal changes arise in this wavelength range (Figure 1a). These changes in CD spectra are indicative of interactions between peptide and the TAR RNA hairpin. A decrease in the intensities of both the positive band at 265 nm and the negative band at 240 nm was observed upon gradual increment of the peptide concentration in the solution. The 265 nm peak is sensitive to base stacking. The decrease in intensity upon forming the complex can be interpreted as a modification of the base stacking induced by the binding of the peptide. In unbound TAR, the three bulge nucleotides are at least partially stacked between the A-form RNA helices which get destacked upon complex formation. This result is consistent with NMR studies of the TAR−Tat complex[6,8] where it is shown that upon peptide binding the stacking of bulge base U23 on A22 and C24 on U23 is disrupted, and A22 becomes juxtaposed to G26 creating an arginine binding pocket. The titration curve at 265 nm, extracted from the CD spectra shown in Figure 1a, is presented in Figure 1b. The total peptide concentration that corresponds to the observed inflection point provides an estimate of the stoichiometry of approximately one Tat peptide molecule per TAR RNA hairpin.

UV Melting Studies. UV melting experiments were carried out to examine the thermal stability of the TAR RNA hairpin in the absence and presence of varying amounts of Tat peptide. Figure 2a shows the UV melting curves for the TAR RNA hairpin duplex in the absence and presence of the peptide, at a peptide to RNA ratio of 0, 1:1, 2:1, and 3:1 in the buffer containing 20 mM Na^+ at pH 7.5. In the absence of peptide, the T_m value of RNA was found to be 57.5 °C. In the presence of peptide, an increase in T_m was clearly observed indicating an increase in the thermal stability of the RNA. The addition of peptide at a [peptide]/[RNA] ratio of 1.0 lead to peptide-induced thermal enhancement (ΔT_m) by 8.5 (±1) °C. Higher [peptide]/[RNA] ratios result in only a marginal increase in the T_m of the RNA hairpin. This marginal increase in the T_m of the RNA at higher ratios is indicative of secondary binding events at high peptide concentrations. The sensitivity of the peptide-induced enhancement in TAR RNA duplex thermal stability (ΔT_m) to salt concentration was further determined by performing similar experiments under different salt concentrations of 40 and 80 mM Na^+. As observed from Figure 2b and 2c, the extent of change in melting temperature (ΔT_m) is highly sensitive to Na^+ concentration. As can be seen, raising the Na^+

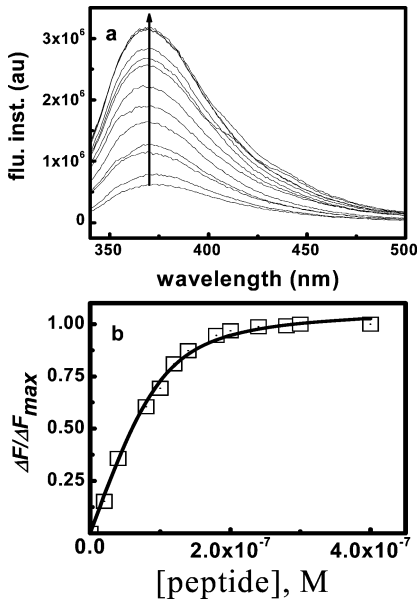

Figure 3. (a) Fluorescence spectra of the Tat peptide−AP−TAR RNA complexes, (b) fluorescence titration curves of several [peptide]/[RNA] ratios detected at 370 nm in buffer consisting of 10 mM sodium cacodylate, 10 mM NaCl, and 0.1 mM NaEDTA, at pH 7.5 and 25 °C. [AP−TAR RNA] = 0.1 μM. Solid lines represent fits of the experimental data points with eq 3. Solution conditions were 10 mM sodium cacodylate (pH 7.5) and 0.1 mM NaEDTA, and NaCl was added to achieve total Na^+ concentration of 20 mM. The fluorescence emission intensity at 370 nm (F_{370}) was normalized by subtraction of the fluorescence intensity in the absence of drug ($\Delta F = F - F_0$) and subsequent division by the total calculated binding-induced change in fluorescence ($\Delta F_{max} = F_{max} - F_0$).

concentration from 20 to 80 mM decreases the peptide-induced ΔT_m from 8.5 to 3.0 °C. A similar observation was made by Kaul et al.[26] in the case of aminoglycoside-rRNA recognition. UV melting experiments at high salt concentration showed no further increase in T_m beyond a [peptide]/[RNA] ratio of 1:1 indicating that the increase was due to nonspecific electrostatic interactions at higher peptide concentration.

Determination of Binding Constants by Fluorescence Titrations. To determine the binding affinity of TAR RNA hairpin duplex−Tat peptide interactions, fluorescence emission spectra of the TAR RNA hairpin duplex in the absence and presence of varying amounts of peptide were recorded. The TAR RNA was fluorescently labeled with 2-aminopurine (2-AP) which was incorporated between two adjacent bulge bases (C and U) in the 27-base fragment of the TAR hairpin. It has been shown earlier that such incorporation of 2-AP bases does not alter the structure of the RNA duplexes or the affinity of peptide for the duplexes.[27–29] TAR RNA hairpin duplex (0.1 μM) was titrated against an increasing concentration of peptide (Figure 3a). It has been shown that changes in the conformation of TAR that accompanies peptide binding at or near the trinucleotide bulge yield changes in 2-AP fluorescence that provide sensitive signals for quantitatively measuring these interactions.[27] Fluorescence intensity was found to increase with increasing peptide concentration as shown in Figure 3a. This increase is indicative of peptide binding as these spectral changes arise from a decrease in stacking and exposure of the bulge AP bases to the aqueous environment.[30] The change in fluorescence intensity at 377 nm was used to construct the binding isotherm (Figure 3b). Analysis of this isotherm following 1:1 binding stoichiometry using eq 3 as described in the experimental procedure yields binding affinities of 8.06 (±0.35) × 10^7 in 20 mM Na^+

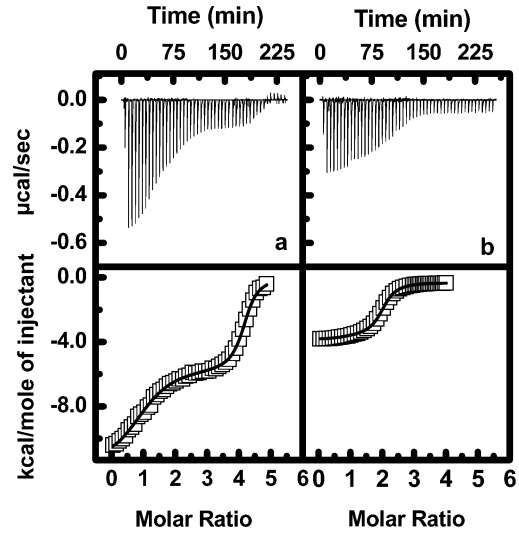

Figure 4. ITC for the binding of Tat peptide to TAR RNA at (a) 20 mM and (b) 80 mM Na^+. In each panel, the top plot is the baseline corrected experimental data. For the lower plots, results were converted to molar heats and plotted against the peptide to RNA molar ratio. The same buffer and conditions were used as in Figure 3.

containing buffer at 25 °C. This value is in accordance with the literature value where the dissociation constant of the peptide−RNA pair studied here was measured by gel electrophoresis mobility shift assay and was found to be 600 nM ($1/K_a$).[31]

Isothermal Titration Calorimetry Studies. We used isothermal titration calorimetry (ITC) to characterize the binding of peptide to TAR RNA in 10 mM sodium cacodylate buffer containing 20 and 80 mM Na^+ concentration at pH 7.5. Figure 4 shows representative ITC profiles resulting from the injection of peptide at pH 7.5 into a solution of TAR RNA hairpin duplex. In the upper panels of Figure 4, each of the heat burst curves corresponds to a single peptide injection. The areas under these heat burst curves were determined by integration to yield the associated injection heats. These injection heats were corrected by subtraction of the corresponding dilution heats derived from the injection of identical amounts of peptides into buffer alone. In Figure 4, the bottom panels show the resulting corrected injection heats plotted as a function of the [peptide]/[RNA] ratio. The ITC profile for the binding of the Tat peptide to TAR RNA hairpin duplex is biphasic. The first apparent phase corresponds to the specific binding, and the other apparent phases could arise due to nonspecific binding. Similar observations were also made in the case for aminoglycoside binding to prokaryotic and eukaryotic rRNA A-sites.[32,33] Nonspecific binding can be expected due to the highly positive nature of the peptide that can interact with the RNA backbone through electrostatic interactions. The injection heat data corresponding to the titration of the RNA with peptide at [Na^+] = 20 and 80 mM were fitted with a model for two independent sets of binding sites. The derived parameters from these fits are summarized in Table 1. ITC studies showed that Tat peptide binds to two different sites of TAR RNA with different affinities indicating the presence of two binding equilibria having values of 8.01 (±0.1) × 10^7 M^{-1} and 0.70 (±0.25) × 10^7 M^{-1} under the same conditions. As observed from Table 1, the first binding equilibrium is associated with a binding stoichiometry (n) of approximately 1 peptide molecule/RNA. However, the second binding is accompanied with a stoichiometry (n) of 3 and 1 peptide molecules/RNA at 20 and 80 mM Na^+ concentration, respectively. The reduced stoichiometry for the second binding

TABLE 1: ITC-Derived Binding Parameters at 25 °C for the Complexation of TAR RNA with Tat Peptide at pH 7.5 and Na^+ Concentration of 20 and 80 mM[a]

Na^+			ΔH_1[b]	$T\Delta S_1$[c]			ΔH_2[b]	$T\Delta S_2$[c]
mM	n_1[b]	$K_{a1}(M^{-1})$[b] $\times 10^7$	kcal/mol	kcal/mol	n_2[b]	$K_{a2}(M^{-1})$[b] $\times 10^6$	kcal/mol	kcal/mol
20	1.01 ± 0.02	8.01 ± 0.10	-10.5 ± 0.3	2.8 ± 0.3	$3.3.0 \pm 0.02$	7.01 ± 0.62	-5.5 ± 0.1	3.9 ± 0.2
80	0.96 ± 0.03	1.74 ± 0.25	-5.5 ± 0.2	4.4 ± 0.3	1.0 ± 0.03	2.31 ± 0.03	-4.2 ± 0.2	4.5 ± 0.3

[a] The values of K, ΔH, ΔS, and n listed here were derived from the fits of the ITC profiles shown in the bottom panels of Figure 4 with a model for two sets of independent binding sites. The indicated uncertainties reflect the standard deviations of the experimental data. [b] Values of K_a, ΔH, and n were derived from fits of ITC data as described in the text, with the indicated uncertainties reflecting the 95% confidence intervals. [c] Values of ΔS were calculated using the standard relationship $\Delta G = \Delta H - T\Delta S$, with the indicated uncertainties reflecting the maximum possible errors in ΔH and ΔG as propagated through this equation.

obtained at 80 mM [Na^+] ion concentration indicates the nonspecific nature of second binding. The enthalpy change associated with the first binding (ΔH_1) is more exothermic at -10.5 ± 0.31 kcal/mol than the enthalpy change associated with the second binding (ΔH_2) at -5.4 ± 0.11 kcal/mol. Moreover, these enthalpy changes associated with both the binding sites are less negative for the binding at higher salt concentration of 80 mM Na^+ with ΔH_1 and ΔH_2 having values -5.5 ± 0.02 and 4.5 ± 0.03 kcal/mol, respectively.

Inspection of Table 1 indicates that specific binding is associated with largely favorable enthalpy change (ΔH_1) and with unfavorable entropy change at low salt (20 mM Na^+) concentration, whereas nonspecific interaction is associated with a considerable amount of favorable enthalpy change (ΔH_2) as well as favorable entropy change. At high salt concentration (80 mM Na^+), both the favorable enthalpy change (ΔH) and the favorable entropy change (ΔS) contributed considerably to the overall binding energy. The favorable enthalpy change is associated with the formation of hydrogen bonds and van der Waals contacts, and the unfavorable enthalpy change is associated with the desolvation of polar groups. From several NMR studies on RNA and arginine-rich peptide, it is shown that a network of hydrogen bonds contributes to the stability of the complexes. Obtained exothermic enthalpies for the binding corroborate that the interaction is mainly through hydrogen bond formations between the peptides and RNA. In light of this information, it is reasonable to expect the binding free energy to have a large nonpolyelectrolyte component.

Although there is no such study available in the literature for RNA−peptide interaction, similar observations involving specific and nonspecific bindings were found for the DNA−protein interactions.[34,35] This large effect of salt concentration on ΔH appears to result, at least partly, from the release of preferentially bound anionic counterions of Tat peptide upon binding to TAR RNA. If it is so, then the interaction factor i, which quantifies the linkage between ion release and temperature, should have a positive value, implying that the ion release decreases with increasing temperature and the enthalpy change increases with salt concentration which was observed in the present case.[36] The structural basis of these effects can however not be elucidated with the available data. Further, more detailed studies on Tat peptide−TAR RNA and on other RNA binding peptides are required to fully understand this factor.

Next, binding enthalpy was also obtained from temperature-dependent binding experiments. Fluorescence titrations were also carried out at different temperatures ranging from 10 to 30 °C under similar buffer conditions. By performing these experiments over a range of temperatures, it was possible to determine enthalpy for the binding (ΔH_{vH}) using a form of the van't Hoff equation ($\ln K_a = -(\Delta H_{vH}/RT) + \Delta S/R$). The ΔH_{vH} was calculated to be -8.96 (± 0.48) and -4.09 (± 0.33) kcal/mol from the slope of the plot of ln K versus $1/T$ (Figure 5) at 20 and 80 mM Na^+ salt concentrations. Though enthalpies obtained from the two above said methods are very close to each other, they do not have similar ratios ($\Delta H_{cal}/\Delta H_{vH}$) of 1.17 and 1.27 at 20 and 80 mM Na^+ concentrations, respectively. It has been suggested that the observed discrepancies between ΔH_{cal} and ΔH_{vH} could be due to binding reactions that are more complicated than is suggested by the one-to-one binding scheme used to model the data. A difference between the van't Hoff and calorimetric enthalpies could be due to large temperature-dependent behavior of associated reactions such as displacement of water, counterions, or protons, as well as conformational equilibria, that could be contributing differently to the calorimetric and van't Hoff enthalpies. Some of these phenomena, such as displacement of water and counterions, are already observed for the present system.

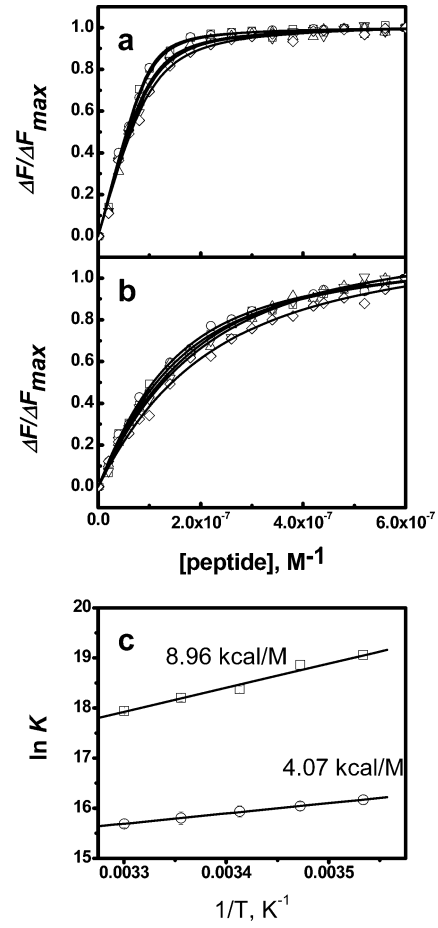

Figure 5. Binding isotherm at (□) 10, (○) 15, (△) 20, (▽) 25, and (◇) 30 °C in the presence of 20 mM (plot a) and 80 mM (plot b) for Tat peptide−AP−TAR RNA interaction. Van't Hoff analysis of the temperature dependence of the equilibrium dissociation constants (plot c) at (□) 20 and (○) 80 mM Na^+. Experiments were done in in 10 mM sodium cacodylate buffer (pH = 7.5).

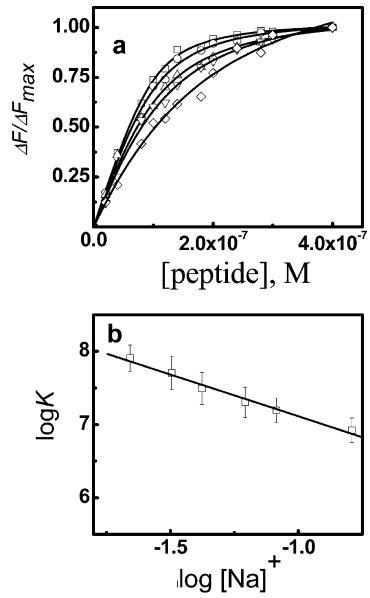

Figure 6. (a) Binding isotherm at (□) 20, (○) 30, (△) 40, (▽) 60, and (◇) 160 mM Na^+. (b) Dependence of equilibrium binding constants for Tat peptide−AP−TAR RNA interaction on the salt concentration. Experiments were done in in 10 mM sodium cacodylate buffer (pH =7.5) at 25 °C. Data are presented as a double-logarithmic plot according to the theory of Record et al.[24] The linear least-squares fit to the data is shown by the solid lines, yielding a slope of 1.14 (±0.07).

Salt Dependence of the Binding Constants. To estimate the involvement of counterions in this binding process as well as to determine the role of electrostatic interactions, titrations were performed in 10 mM sodium cacodylate buffer at 25 °C with Na^+ concentration ranging from 20 to 160 mM at pH 7.5 as shown in Figure 6a. The binding constant (K_a) decreased with increasing Na^+ concentration (Table 2).

Salt effects in nucleic acid systems are often described by models based on Manning's counterion condensation theory.[37] Record et al.[24] incorporated this theory into a thermodynamic description of ligand−DNA interactions. They derived eq 4 to describe the linear salt dependence of the observed association constant. The slope of log K_a versus log[Na^+] is equivalent to the number of counterions released upon binding of a ligand with charge Z. The observed free energies of any ligand−nucleic acid interaction can be dissected into contributions from various molecular processes that occur during complex formation.[25] By applying this theory, the observed binding free energy (ΔG_{obs}) can be dissected into two component terms, given in eq 6, ΔG_{pe}, which is the electrostatic (polyelectrolyte) contribution, due mainly to coupled polyelectrolyte effects involving the release of condensed counterions from the nucleic acid upon ligand binding, and ΔG_t, which is the nonpolyelectrolyte contribution; this energetic contribution arises from all other factors including conformational changes upon complex formation, hydrophobic contacts, molecular interactions, like van der Waals forces, dipole−dipole interactions, etc.

Salt dependence was examined by the polyelectrolyte theory using eq 4 as described in the Materials and Methods section. A linear relationship is obtained between log K_a and log[Na^+] for all TAR RNA hairpin duplex and Tat peptide interactions as shown in Figure 6b. The linear plot yielded a slope of −1.14 indicating the release of one counterion upon binding. The observed binding free energy ($\Delta G_{obs} = -RT \ln K_a$) was dissected into its polyelectrolyte (ΔG_{pe}) and nonpolyelectrolyte (ΔG_t) contributions using eq 6. Table 3 summarizes the relative polyelectrolyte and nonpolyelectrolyte contributions to observed free energy change. Owing to the highly charged nature of polyanionic RNA, electrostatics is expected to dominate the binding thermodynamics.The polyelectrolyte contribution arises from a release of counterions from RNA upon ligand binding which is mainly an entropic effect, while the nonpolyelectrolyte contribution arises from other molecular interactions like hydrogen bond and van der Waal interactions. Previous thermodynamic studies of positively charged oligopeptides binding to both single-stranded and duplex DNA and RNA have demonstrated that the major driving force for forming such complexes results from the release of cations bound to these nucleic acids which is mainly an entropic effect.[38–41] However, the salt dependence study as shown in Table 2 indicates that electrostatic interaction contributes only to a limited extent in the free energy change, the major role being played by nonpolyelectrolyte interactions. Release of only one counterion suggests that only one NH_3^+ group is involved in the interaction. Out of the six arginine molecules present in the peptide, only one arginine is involved in electrostatic interaction with the TAR RNA. NMR studies on HIV-1 TAR RNA[6,8] have shown that the RNA changes conformation in response to peptide binding, and an argininеamide induces a similar change mainly through hydrogen bonds, although a higher concentration is required than for the peptide. It has also been shown that arginine, present as free amino acid, binds TAR with specificity similar to Tat peptide,[42,43] underscoring the role of a critical arginine residue in the TAR−Tat interaction.

As can be seen from the data presented in Table 2, ΔG_{pe} or the polyelectrolyte binding free energy that arises from the binding-induced release of condensed counterions contributes only marginally to the binding free energy. The majority of the contribution to the Gibbs free energy comes from nonpolyelectrolyte sources.

Therefore, the salt-dependent study shows that one arginine is involved in ionic interaction, the major role in binding being played by hydrogen bonding particularly by a single critical arginine making specific contacts with TAR RNA. Although the exact role of other arginines cannot be concluded from this study, it can be stated that the rest of the arginines are not involved in ionic interaction. The other arginines can be involved in hydrogen bonding due to their high hydrogen bonding potential. However, the relative contribution of other arginines in the binding process can be obtained by mutating these residues systematically and observing the change in the thermodynamic profile of binding. In a similar study involving certain zing finger proteins and HIV RREIIB RNA, it was found that the extent of electrostatic contributions to the binding free energy was much less than expected and was largely driven by favorable interaction at the major groove rather than the phosphate backbone.[44]

Osmotic Stress Dependence of the Binding Constants. In search of discrepancies between ΔH_{cal} and ΔH_{Vh}, we sought to understand the involvement of water molecules in the binding process. The number of water molecules released or taken up by the formation of a complex between the peptide and RNA duplex can be estimated by examining the effects on the binding affinity upon alteration of water activity using neutral solutes to vary the osmotic strength.[45–47] The osmotic stress method has been extensively used to monitor the hydration changes accompanying different biomolecular interactions. Osmotic stress measurements can reveal the influence of water activity on macromolecular reactions and conformational transactions. The method involves applying osmotic pressure to the system

TABLE 2: Binding Constants (K, M^{-1}) of TAR RNA and Peptide under Different Salt Concentration[a,b]

Na^+, (mM)	20	30	40	60	80	160
K_a (M^{-1}) × 10^7	8.06 ± 0.35	5.08 ± 0.31	3.10 ± 0.25	2.00 ± 0.19	1.71 ± 0.21	0.84 ± 0.09

[a] The binding constants were determined by fluorescence titration experiments in solutions buffered to pH 7.5 with 10 mM sodium cacodylate, containing 0.1 mM NaEDTA. The concentration of Na^+ ranged from 20 to 160 mM. [b] Values of K_a were derived from fluorescence titration experiments as described in the text, with the indicated uncertainties reflecting the 95% confidence intervals.

TABLE 3: Dissection of ΔG_{obs} (kcal/mol) into ΔG_{pe} (kcal/mol) and ΔG_t (kcal/mol)

$[Na^+]$ (M)	ΔG_{obs}[a] kcal/mol	ΔG_{pe} kcal/mol	ΔG_t[b] kcal/mol
20	−10.70	−2.79	−7.95
30	−10.50	−2.50	−7.97
40	−10.20	−2.30	−7.88
60	−9.92	−2.01	−7.91
80	−9.86	−1.92	−7.94
160	−9.40	−1.31	−8.10

[a] Values of ΔG were determined using the standard relationship $\Delta G = RT \ln K_a$, with uncertainty of ±10% reflecting the maximum possible errors in K_a as propagated through this equation. [b] Values of ΔG_{pe} and ΔG_t were calculated using eq 5 and 6, respectively, with uncertainty of ±10% reflecting the maximum possible errors in SK as propagated through these equations.

by adding neutral solutes or osmolytes which otherwise do not interact with the system of interest. These solutes are preferentially excluded from the vicinity of the substrate and lower the activity of water outside the zone of exclusion facilitating the removal of water molecule toward the higher osmotic pressure of the bulk solvent. Thus, if there is a significant number of water molecules associated with the macromolecule surface, equilibria that involve changes in surface exposure become sensitive to changes in the water activity induced by the cosolutes. Therefore, a study of the dependence of the equilibrium constant on water activity can be used to determine the changes in the number of water molecules involved in the equilibrium reaction. The number of water molecules participating in the binding event can be quantified by the equation

$$\delta \ln(K/K_0)/\delta[\mathrm{Osm}] = -\Delta n_w/55.6 \qquad (7)$$

where $\ln(K/K_0)$ is the change in the binding free energy; Osm is the osmolality (moles of solute/kg of solvent) of the solution; and Δn_w is the difference in the number of bound water molecules between the complex and the free reactants.[47]

We used the osmotic stress method to characterize the hydration changes that accompany the binding of the peptide to the RNA duplex using ethylene glycol as an osmolyte. Its molecular weight is sufficiently small relative to that of peptide which minimizes the potential for the introduction of volume exclusion effects. Besides, it has been used successfully to study water uptake or release in different biological processes. Although the secondary structure of TAR RNA remains unaffected in the presence of ethylene glycol at the maximum osmolality used in the osmotic stress studies, it reduces the thermal stability of the TAR RNA hairpin duplex, as revealed by CD and UV melting studies, respectively (data not shown). However, at 25 °C no fraction of unfolded TAR RNA was observed, and thus experiments were performed at this temperature only. Figure 7a and 7b show binding isotherms for the titration of peptide into a solution of TAR RNA hairpin duplex in the absence and presence of ethylene glycol at different osmolality. Analysis of these isotherms using eq 3 described in

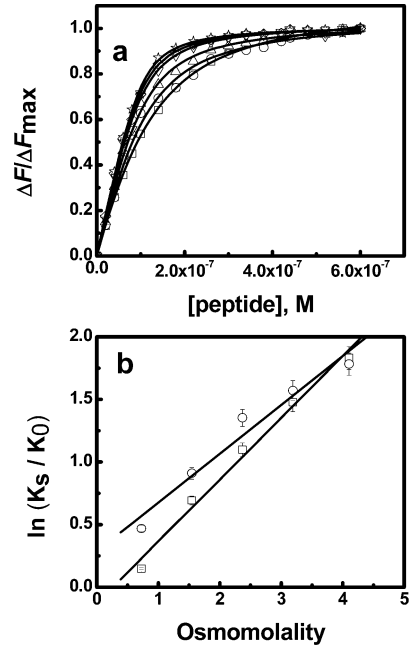

Figure 7. (a) Binding isotherm in the presence of (□) 0, (○) 5, (△) 10, (▽) 15, (◇) 20, and (☆) 25% (w/v) of ethylene glycol at 80 mM Na^+. (b) The natural logarithm plot of the ratio of the binding constant at a given osmolyte concentration (K_s) relative to the binding constant (K_O) versus osmolality in the presence of 20 (□) and 80 (○) mM Na^+. Experiments were done in in 10 mM sodium cacodylate buffer (pH =7.5) at 25°.

the Materials and Methods section revealed that binding affinity (K_a) increases with increase in osmolality of the solution (Figure 7c). An osmolyte-induced increase in K_a indicates a net release of water molecules in conjunction with binding.[48] The change in the binding affinity upon change in osmolyte concentration is shown in Figure 7b. The calculated average number of water molecules released was found to be 27 ± 4 and 21 ± 3 at 20 and 80 mM Na^+ ion concentrations, respectively.

Water is essential for the stability of the highly charged double helix. Ligand binding resulting in removal of waters from the vicinity of RNA must overcome the strong desolvation electrostatics. Thus, the contribution of overall electrostatics to the binding energy, though favorable, is very low in this case. There are two major contributors to the intrinsic binding enthalpy: the favorable enthalpy associated with the formation of hydrogen bonds and van der Waal's contacts and the unfavorable enthalpy associated with the desolvation of polar groups. Therefore, a favorable enthalpy is an indication that the peptide establishes good interactions with the target and that the interactions are strong enough to compensate the unfavorable enthalpy associated with desolvation. TAR−Tat interaction, being enthalpically driven, derives most of its energy from hydrogen bonds, which are stereochemically specific and increase selectivity besides contributing to binding affinity. Certainly, arginine is unique in being positively charged and having the ability to form a pentadentate hydrogen bond. Moreover, all the bindings are also favored by an entropic factor also. The overall positive entropy

term observed in the present system may be due to the release of structured water from the binding site of RNA and/or the peptide itself into bulk solvent and/or the release of condensed counterions upon ligand binding. The release of water molecules upon complex formation supports the positive entropy contribution.

It would be expected that the enthalpy for binding of RNA with peptide is independent of salt concentration; however, our ITC data show that the thermodynamic parameters are salt dependent. This can be attributed to preferential interactions of anions, protons, and water with the peptide along with preferential interaction of cations with TAR RNA. The changes in thermodynamic parameters can also be attributed to hydration changes that accompany peptide−RNA binding. Osmotic stress studies reveal the release of 27 ± 4 and 21 ± 3 at 20 and 80 mM Na^+ ion concentrations, respectively. The binding enthalpy of a ligand that displaces more water molecules from the macromolecular cavity is less exothermic. However, in our study, ΔH for the 20 mM Na^+ ion is found to be more negative than that for the 80 mM Na^+ ion concentrations. This discrepancy can be due to inefficiency of the osmotic stress method in measuring the overall hydration change as shown in other studies.[49] Besides, as mentioned earlier, the effect of preferential binding of an anion to a peptide along with contribution of protonation coupling to anion binding can be explored to identify reasons for the effect of salt on binding enthalpy.

Conclusion

Studying RNA−protein interaction is crucial to understand the basic principles involved in these interactions. In addition, RNA and RNA−protein complexes represent attractive targets for new drug therapies aimed at treating retroviral infections. The interaction between TAR and the HIV-1 protein Tat is essential for virus replication and represents an important target for antiviral therapies. Besides this, it is also a good model system to understand the energetics of RNA−protein interaction because of its simplicity. The studies reported here are initial steps toward establishing the thermodynamic database needed to understand the molecular forces that govern peptide recognition of RNA. Such information will facilitate the rational design of peptides as potential drugs and help predict their sequence and structure-dependent affinities and specificities. Specific alterations in peptide sequence as well as RNA sequence and structure would lead to changes in binding affinities that will provide an in-depth understanding of the factors that govern these interactions. Modifications that yield higher binding affinity toward the target and lesser binding affinity toward other structures are of particular interest.

Acknowledgment. This work was supported by Council of Scientific and Industrial Research (CSIR) (Project title: Comparative Genomics and Biology of noncoding RNA), India. H. Suryawanshi acknowledges a research fellowship from CSIR.

References and Notes

(1) Lazinski, D.; Grzadzelska, E.; Das, A. Sequence-specific recognition of RNA hairpins by bacteriophage antiterminators requires a conserved arginine rich motif. *Cell* **1989**, *59*, 207–218.

(2) Narayana, N.; Weiss, M. A. RNA recognition by arginine-rich peptide motifs. *Biopolymers* **1999**, *48*, 167–180.

(3) Draper, D. E. Themes in RNA-protein recognition. *J. Mol. Biol.* **1999**, *293*, 255–270.

(4) Kenan, D. J.; Query, C. C.; Keene, J. D. RNA recognition: towards identifying determinants of specificity. *Trends Biochem. Sci.* **1991**, *16*, 214–220.

(5) Mattaj, I. W. RNA recognition: a family matter? *Cell* **1993**, *73*, 837–840.

(6) Puglisi, J. D.; Tan, R.; Calnan, B. J.; Frankel, A. D.; Williamson, J. R. Conformation of the TAR RNA-arginine complex by NMR spectroscopy. *Science* **1992**, *257*, 76–80.

(7) Long, K. S.; Crothers, D. M. Characterization of the solution conformations of unbound and Tat peptide-bound forms of HIV-1 TAR RNA. *Biochemistry* **1999**, *38*, 10059–10069.

(8) Aboul-ela, F.; Karn, J.; Varani, G. The structure of the human immunodeficiency virus type-1 TAR RNA reveals principles of RNA recognition by Tat protein. *J. Mol. Biol.* **1995**, *253*, 313–332.

(9) Puglisi, J. D.; Chen, L.; Blanchard, S.; Frankel, A. D. Solution structure of a bovine immunodeficiency virus Tat-TAR peptide-RNA complex. *Science* **1995**, *270*, 1200–1203.

(10) Ye, X.; Kumar, R. A.; Patel, D. J. Molecular recognition in the bovine immunodeficiency virus Tat peptide-TAR RNA complex. *Chem. Biol.* **1995**, *2*, 827–840.

(11) Jiang, F.; Gorin, A.; Hu, W.; Majumdar, A.; Baskerville, S.; Xu, W.; Ellington, A.; Patel, D. J. Anchoring an extended HTLV-1 Rex peptide within an RNA major groove containing junctional base triples. *Structure* **1999**, *7*, 1461–1472.

(12) Ye, X.; Gorin, A.; Ellington, A. D.; Patel, D. J. Deep penetration of an alphahelix into a widened RNA major groove in the HIV-1 rev peptide-RNA aptamer complex. *Nat. Struct. Biol.* **1996**, *3*, 1026–1033.

(13) Bayer, P.; Kraft, M.; Ejchart, A.; Westendorp, M.; Frank, R.; Rosch, P. Structural studies of HIV-1 Tat protein. *J. Mol. Biol.* **1995**, *247*, 529–535.

(14) Legault, P.; Li, J.; Mogridge, J.; Kay, L. E.; Greenblatt, J. NMR structure of the bacteriophage lambda N peptide/boxB RNA complex recognition of a GNRA fold by an arginine-rich motif. *Cell* **1998**, *93*, 289–299.

(15) Cai, Z.; Gorin, A.; Frederick, R.; Ye, X.; Hu, W.; Majumdar, A.; Kettani, A.; Patel, D. J. Solution structure of P22 transcriptional antitermination N peptide-box B RNA complex. *Nat. Struct. Biol.* **1998**, *5*, 203–212.

(16) Battiste, J. L.; Mao, H.; Rao, N. S.; Tan, R.; Muhandiram, D. R.; Kay, L. E.; Frankel, A. D.; Williamson, J. R. Alpha helix major groove recognition in an HIV-1 Rev peptide-RRE RNA complex. *Science* **1996**, *273*, 1547–1551.

(17) Ye, X.; Gorin, A.; Frederick, R.; Hu, W.; Majumdar, A.; Xu, W.; McLendon, G.; Ellington, A.; Patel, D. J. RNA architecture dictates the conformations of a bound peptide. *Chem. Biol.* **1999**, *6*, 657–669.

(18) Brodsky, A. S.; Williamson, J. R. Structure of HIV-2 TAR-argininamide complex. *J. Mol. Biol.* **1997**, *267*, 624–639.

(19) Yang, Y.; Kochoyan, M.; Burgstaller, P.; Westhof, E.; Famulok, M. Structural basis of ligand discrimination by two related RNA aptamers resolved by NMR spectroscopy. *Science* **1996**, *272*, 1343–1347.

(20) Churcher, M. J.; Lamont, C.; Hamy, F.; Dingwall, C.; Green, S. M.; Lowe, A. D.; Butler, J. G.; Gait, M. J.; Karn, J. High Affinity Binding of TAR RNA by the Human Immunodeficiency Virus Type-1 *Tat* Protein Requires Base-pairs in the RNA Stem and Amino Acid Residues Flanking the Basic Region. *J. Mol. Biol.* **1993**, *230*, 90–110.

(21) Harrich, D.; Ulich, C.; Garcia-Martinez, L. F.; Gaynor, R. B. Tat is required for efficient HIV-1 reverse transcription. *EMBO J.* **1997**, *16*, 1224–1235.

(22) Marky, L. A.; Blumenfeld, K. S.; Kozlowski, S.; Breslauer, K. J. Salt-dependent conformational transitions in the self-complementary deoxydodecanucleotide d(CGCAATTCGCG):evidence for hairpin formation. *Biopolymers* **1983**, *22*, 1247–1257.

(23) Marky, L. A.; Breslauer, K. J. Calculating thermodynamic data for transitions of any molecularity from equilibrium melting curves. *Biopolymers* **1987**, *26*, 1601–1620.

(24) Record, M. T.; Anderson, C. F.; Lohman, T. M. Thermodynamic analysis of ion effects on the binding and conformational equilibria of proteins and nucleic acids: the roles of ion association or release, screening, and ion effects on water activity. *Q. Rev. Biophys.* **1978**, *11*, 103–178.

(25) Chaires, J. B.; Dissecting the free energy of drug binding to, D. N. A. *Anti-Cancer Drug Des.* **1996**, *11*, 569–580.

(26) Kaul, M.; Pilch, D. Thermodynamics of aminoglycoside-rRNA recognition: the binding of neomycin-class aminoglycosides to the A site of 16S rRNA. *Biochemistry* **2002**, *41*, 7695–7706.

(27) Bradrick, T. D.; Marino, J. P. Ligand induced changes in 2-aminopurine fluorescence as a probe for small molecules binding to HIV-1 TAR RNA. *RNA* **2004**, *10*, 1459–1468.

(28) Austin, R. J.; Xia, T. B.; Ren, J. S.; Takahashi, T. T.; Roberts, R. W. Differential modes of recognition in N peptide-boxB complexes. *Biochemistry* **2003**, *42*, 14957–14967.

(29) Barrick, J. E.; Roberts, R. W. Achieving specificity in selected and wild-type N peptide-RNA complexes: The importance of discrimination against noncognate RNA targets. *Biochemistry* **2003**, *42*, 12998–13007.

(30) Rist, M.; Marino, J. P. Fluorescent nucleotide base analogs as probes of nucleic acid structure, dynamics and interactions. *Curr. Org. Chem.* **2001**, *6*, 775–793.

(31) Bayer, T. S.; Booth, L. N.; Knudsen, S. M.; Ellington, A. D. Arginine-rich motifs present multiple interfaces for specific binding by RNA. *RNA* **2005**, *11*, 1848–1857.

(32) Barbieri, C. M.; Kerrigan, J. E.; Pilch, D. S. Coupling of drug protonation to the specific binding of aminoglycosides to the A site of 16 S rRNA: elucidation of the number of drug amino groups involved and their identities. *J. Mol. Biol.* **2003**, *326*, 1373–1387.

(33) Kaul, M.; Barbieri, C. M.; Pilch, D. S. Fluorescence-based approach for detecting and characterizing antibiotic-induced conformational changes in ribosomal RNA: comparing aminoglycoside binding to prokaryotic and eukaryotic ribosomal RNA sequences. *J. Am. Chem. Soc.* **2004**, *126*, 3447–3453.

(34) Holbrook, J. A.; Tsodikov, O. V.; Saecker, R. M.; Record, M. T., Jr. Specific and nonspecific interactions of integration host factor with DNA: thermodynamic evidence for disruption of multiple IHF surface salt-bridges coupled to DNA binding. *J. Mol. Biol.* **2001**, *310*, 379–401.

(35) Oda, M.; Furukawa, K.; Ogata, K.; Sarai, A.; Nakamura, H. Thermodynamics of specific and nonspecific DNA binding by the c-Myb DNA-binding domain. *J. Mol. Biol.* **1998**, *276*, 571–590.

(36) Lohman, T. M.; Overman, L. B.; Ferrari, M. E.; Kozlov, A. G. A highly salt-dependent enthalpy change for Escherichia coli SSB protein-nucleic acid binding due to ion-protein interactions. *Biochemistry* **1996**, *35*, 5272–5279.

(37) Manning, G. S. Limiting laws and counterion condensation in polyelectrolyte solution. I. Colligative properties. *J. Chem. Phys.* **1969**, *51*, 924–933.

(38) Record, M. T., Jr.; Lohman, M. L.; De Haseth, P. Ion effects on ligand-nucleic acid interaction. *J. Mol. Biol.* **1976**, *107*, 145–158.

(39) Mascotti, D. P.; Lohman, T. M. Thermodynamic extent of counterion release upon binding oligolysines to single-stranded nucleic acids. *Proc. Natl. Acad. Sci. U.S.A.* **1990**, *87*, 3142–3146.

(40) Mascotti, D. P.; Lohman, T. M. Thermodynamics of Single Stranded RNA Binding to Oligolysines Containing Tryptophan. *Biochemistry* **1992**, *31*, 8932–8946.

(41) Mascotti, D. P.; Lohman, T. M. Thermodynamics of Single Stranded RNA and DNA Interactions with Oligolysines Containing Tryptophan. Effects of Base Composition. *Biochemistry* **1993**, *32*, 10568–10579.

(42) Calnan, B. J.; Biancalana, S.; Hudson, D.; Frankel, A. D. Analysis of arginine-rich peptides from the HIV Tat protein reveals unusual features of RNA-protein recognition. *Genes Dev.* **1991**, *5*, 201–210.

(43) Tao, J.; Frankel, A. D. Specific binding of arginine to TAR RNA. *Proc. Natl. Acad. Sci. U.S.A.* **1992**, *89*, 2723–2726.

(44) Mishra, S. H.; Spring, A. M.; German, M. W. Thermodynamic profiling of HIV RREIIB RNA-Zinc finger interactions. *J. Mol. Biol.* **2009**, *393*, 369–382.

(45) Haq, I.; Jenkins, T. C.; Chowdhry, B. Z.; Ren, J.; Chaires, J. B. Parsing free energies of ligand-DNA interactions. *Methods Enzymol.* **2000**, *323*, 373–405.

(46) Robinson, C. R.; Sligar, S. G. Hydrostatic and osmotic pressure as tools to study macromolecular recognition. *Methods Enzymol.* **1995**, *259*, 395–427.

(47) Parsegian, V. A.; Rand, R. P.; Rau, D. C. Macromolecules and water: probing with osmotic stress. *Methods Enzymol.* **1995**, *259*, 43–94.

(48) Record, M. T. Jr.; Ha, J. H.; Fisher, M. A. Analysis of Equilibrium and Kinetic Measurements to Determine the Thermodynamic Origins of Stability and Specificity and Mechanism of Formation of Site Specific Complexes Between Proteins and Helical DNA. *Methods Enzymol.* **1991**, *208*, 291–343.

(49) Chaires, J. B. A thermodynamic signature for ligand-DNA binding mode. *Arch. Biochem. Biophys.* **2006**, *453*, 26–31.

JP1000545